Available online at www.sciencedirect.com
SCIENCE DIRECT
Journal of Crystal Growth 287 (2006) 354–358
JOURNAL OF CRYSTAL GROWTH
www.elsevier.com/locate/jcrysgro

Study of carrier localization in InGaN/GaN quantum well blue-light-emitting diode structures

J.H. Chen[a], Z.C. Feng[a,*], J.C. Wang[a], H.L. Tsai[b], J.R. Yang[b], A. Parekh[c], E. Armour[c], P. Faniano[c]

[a]*Graduate Institute of Electro-Optical Engineering and Department of Electrical Engineering, National Taiwan University, Taipei 106-17, Taiwan, ROC*
[b]*Department of Material Science & Engineering, National Taiwan University, Taipei 106-17, Taiwan, ROC*
[c]*Veeco TurboDisc Operations, 394 Elizabeth Ave., Somerset, NJ 08873, USA*

Abstract

The effect of temperature and excitation power on the characteristics of InGaN/GaN single quantum well (SQW) and multiple quantum well (MQW) light-emitting diodes (LED) has been investigated in-depth over a broad range of temperatures from 9 to 300 K. It was found that the device with a stair-shaped SQW structure exhibited stronger localization effect, as well as had higher internal quantum efficiency than that of the conventional MQW and SQW LEDs. This is interpreted as due to the stair-shaped SQW configuration, which offered a large contribution to the exciton capturing. The adoption of an appropriate heterostructure in active region allows the achievement of improved LED performance. With increasing the excitation power intensity, QW photoluminescence (PL) line broadening and emission peak blue shifts were observed, which are assumed to be caused by the disordering formed in the In-rich heterostructures of QW ensembles. We expect that distinct degree of carrier localization occurs in these samples.

PACS: 68.37.Lp; 78.55.Cr; 81.05.Ea; 81.15.Gh

Keywords: A1. Luminescence; B1. InGaN; B3. MQW-LED; B3. SQW-LED

1. Introduction

InGaN-based semiconductors have recently attracted much attention, especially for their light-emitting device application, such as high-brightness light-emitting diodes (LEDs) and continue-wave (cw) blue laser diodes (LDs). Large lattice mismatch and thermal expansion coefficient mismatch between the sapphire substrate and the epitaxial layers result in high density of defects, primarily threading dislocations of up to $10^{10}\,cm^{-2}$ through the InGaN/GaN multiple quantum wells (MQWs). However, the luminescent efficiency of these QW devices is surprisingly high. Recently, evidences from cathodoluminescence (CL) [1], transmission electron microscopy (TEM) [2,3] and near-field scanning optical microscopy [4] have indicated the formation of quantum dot (QD)-like structures due to the nonuniform distribution of indium inside the InGaN well region, leading to potential minima for localized carrier recombination. The performance of some optical devices based on InGaN/GaN quantum heterostructures can thus be greatly improved owing to the three-dimensional (3D) confinement of electrons and holes in QD-like regions. On the other hand, their optical properties are strongly affected by the quantum-confined-Stark effect (QCSE) due to the presence of a large piezoelectric field in the quantum well, which arises from strain caused by the lattice mismatch between GaN and InGaN [5,6]. In this paper, we report on three InGaN/GaN QW LED wafers with different structures and investigate their optical and structural characteristics.

2. Sample and experiment

Three samples were characterized in this study. These high-quality InGaN/GaN quantum well LED wafers were

*Corresponding author. Tel.: +886 223 63 5251; fax: +886 223 67 7467.
E-mail address: zcfeng@cc.ee.ntu.edu.tw (Z.C. Feng).

0022-0248/$ - see front matter © 2005 Elsevier B.V. All rights reserved.
doi:10.1016/j.jcrysgro.2005.11.043

grown on (0 0 0 1)-plane sapphire substrates by low-pressure (LP) metalorganic chemical vapor deposition (MOCVD) using an Emcore system with the vertical growth configuration and a high-speed rotation disk, i.e. the so-called Turbo-disc technology. Trimethylgallium (TMGa), trimethylindium (TMIn), and ammonia (NH_3) were used as precursors for Ga, In, and N, respectively. The carrier gases were H_2 and N_2, respectively, for the growth of GaN and InGaN. For the growth procedures, the substrates are initially treated in H_2 ambient at 1173 °C, followed by the growth of a 25 nm thick low-temperature (550 °C) GaN buffer layer and a 3 μm thick layer of Si-doped GaN grown at high temperature (1020 °C) under low pressure. Afterwards, the temperature was lowered to grow InGaN/GaN quantum wells layer. One sample, which was labeled 4-QWs, consists of four periods of InGaN/GaN MQWs sandwiched between n-GaN doped with Si and p-type GaN doped with Mg. Another sample, labeled single quantum well (SQW), contains only one QW sandwiched between n-type GaN and p-type GaN. Furthermore, the other sample, labeled stair-shaped SQW, contains one well sandwiched between n-type GaN and p-type AlGaN, and stair shape of InGaN QW was formed by controlling the indium composition with time during the well growth.

Structural analysis was carried out by high-resolution transmission electron microscopy (HR-TEM) bright field images and the atomic resolved high-angle angular dark field (HAADF) scanning TEM images. The specimen for TEM observations were mechanically polished into a wedge shape by using a Tripod polisher, followed by Ar^+ ion milled at 5.0 kV to electron transparency in a Gatan Model 691 precision ion polishing system (PIPS). The prepared TEM specimen was examined with a Philips Tecnai F30 field-emission-gun electron microscope, equipped with a dark-field annular detector, operated at 300 kV.

For the photoluminescence (PL) experiments, a cw He-Cd laser ($\lambda = 325$ nm) was used for PL excitation and a neutral density filter was used for controlling the excitation intensity. The samples to be measured were placed in a cryostat to control the ambient temperature. With circulated liquid helium, the cryostat could reach the lowest temperature of ~9 K. The luminescence was dispersed by a 0.85 m monochromator and detected by a water-cooled GaAs photon multiplier interfaced with a lock-in amplifier.

3. Results and discussion

Fig. 1 shows the schematic energy band structures and the HAADF-STEM images for the three QW samples and the structural parameters such as well and barrier thickness were characterized. Their InGaN well thicknesses are all about 2.5 nm. Fig. 2 shows PL spectra of the 4-QWs, SQW, and stair-shaped SQW samples measured at room temperature (300 K) and low temperature (9 K). In each case, the excitation power is fixed about 23 meV. Each spectrum

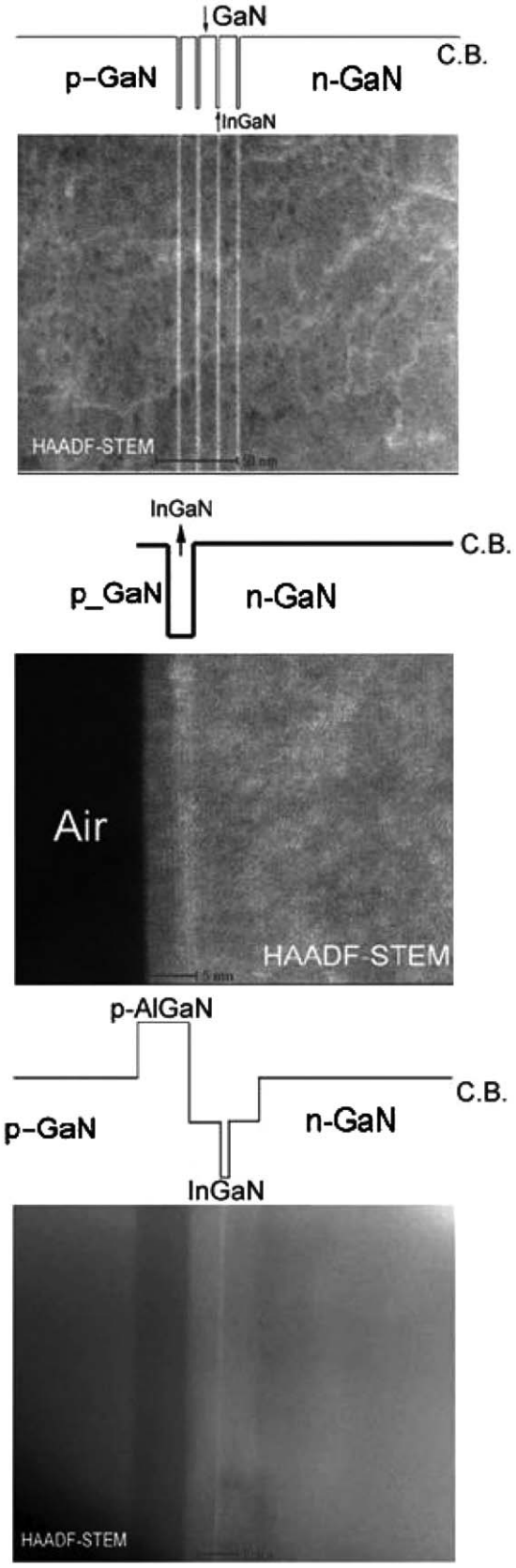

Fig. 1. The schematic energy band structures and the HAADF-STEM images for the three QW samples.

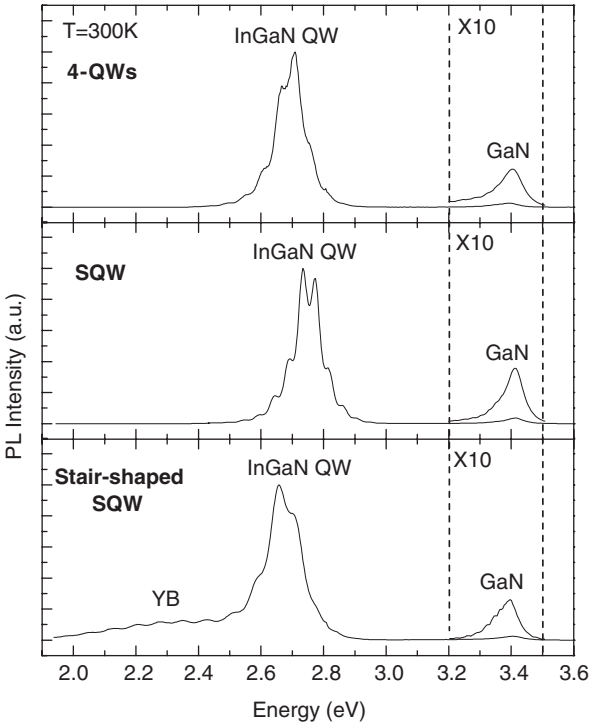

Fig. 2. The PL spectra of the 4-QWs, SQW, and stair-shaped SQW samples measured at 9 and 300 K.

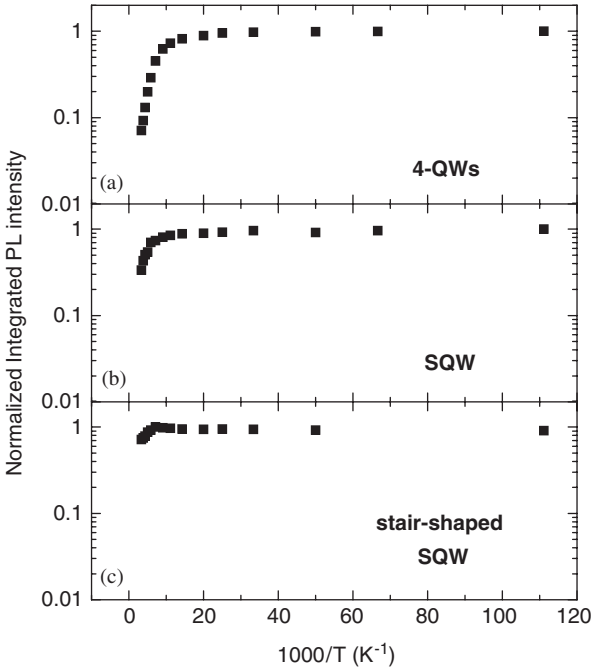

Fig. 3. The temperature dependence of the normalized integrated PL intensity in the form of an Arrhenius plot, i.e. $\log(I(T))$ versus $1000/T$, of the InGaN/GaN 4-QWs, SQW, and stair-shaped SQW samples.

is dominated by a strong emission band with a weak peak. The strong emission between 2.5 and 2.9 eV is interpreted due to the InGaN quantum well transition and the weak peak near 3.4 eV is from the GaN barrier. It is noted that the yellow emission band (YB) located at about 2.3 eV was clearly observed in the 4-QWs sample but was not obvious in other samples. It means that the quality of the GaN barrier layers for 4-QWs sample is poorer than that for SQW and stair-shaped SQW samples. This point is reasonable if the process of the growth is considered. Generally, the growth temperature of InGaN is much lower than that of GaN. The first InGaN well is deposited on the surface of high-quality GaN layer, which is grown at high temperature. But the subsequent InGaN wells are deposited on the GaN layer grown at the low temperature, which is the same as the growth temperature of InGaN. In addition, during MQW growth, N_2 as a carrier gas was used instead of H_2 in order to enhance the indium incorporation.

Figs. 3(a)–(c) show the temperature dependence of the normalized integrated PL intensity in the form of an Arrhenius plot, i.e. $\log(I(T))$ versus $1000/T$, of the InGaN/GaN 4-QWs, SQW, and stair-shaped SQW samples, respectively. For the 4-QWs sample, the integrated PL intensity falls gradually with increasing temperature due to increasing nonradiative recombination pathway. However, in the SQW sample case, the integrated PL intensity falls gradually, except when there is a slight raise in the temperature of about 20–30 K. Furthermore, for the stair-shaped SQW sample, the integrated PL intensity increases up to 140 K first; then decreases with increasing temperature. Such behaviors are quite different from previous results [7,8]. The anomalous phenomenon can be attributed to carrier supply with thermal energy. With thermal energy, carriers can overcome certain potential barriers and relax into localized states formed by the InGaN clusters. In addition, for these cases, the integrated PL intensity cannot be well fitted using the one-activation energy Arrhenius formula as: $I(T) = I_0/[1 + \alpha \exp(-E_A/k_B T)]$. We use the relationship applied to amorphous semiconductors and disordered superlattices as: $I(T) = I_0/[1 + A \exp(T/T_0)]$ [9,10]. Here, I is the PL intensity, T is the temperature, and T_0 is the characteristic temperature corresponding to the energy depth of localized states from a mobility edge. A is the tunneling factor and I_0 is the luminescence intensity at the low-temperature limit. From the fitting, A/T_0 are calculated to be 0.106/52.968 K, 0.127/103.1 K, and 0.146/398 K for the InGaN/GaN 4-QWs, SQW, and stair-shaped SQW samples, respectively. Comparing the characteristic temperature T_0 among these structures, we can also find T_0 of the stair-shaped SQW structure as the highest and that of the 4-QWs sample as the lowest. It should be noted that the process for self-formation of InGaN QDs like nanostructures may be a result of the intrinsic nature of InGaN ternary alloys since the compositional modulation due to phase separation would be energetically favored in InGaN-based heterosystems. It is likely that the high-quantum efficiency of InGaN-based LEDs is mostly due to the large localization of excitons because the pathways of nonradiative

recombination are hindered once the excitons are captured in a small volume. However, the characteristic temperature relation also responds to the localization energy depth relation among them. Therefore, we expect that the carriers in the stair-shaped SQW sample have the strongest localization effect and that in the 4-QWs sample have the weakest, resulted in higher internal quantum efficiency extracted from PL spectra at room temperature.

Figs. 4(a) and (b) show the excitation power dependence of the emission peak position and linewidth full-width at half-maximum (FWHM) of the three samples. For the 4-QWs sample, the peak position and linewidth of the QW emission remain constant with excitation power increasing. We can assume that both carrier localized band-state filling and excess-carrier-induced screening effects are negligible in the 4-QWs sample under variance excitation power intensities. While comparing with others, such as the SQW and stair-shaped SQW sample, the absence of such a blue shift of peak position and broadening of linewidth in 4-QWs sample indicates the different radiative recombination mechanisms in the three samples. Moreover, it also immediately suggests the presence of the localization states in SQW and stair-shaped SQW sample. The peak position of the QW emission shifts toward shorter wavelengths as the excitation power increases, resulting in about 40 and 27 meV blue shift for the SQW and stair-shaped SQW samples, respectively, as the excitation power is increased from 0.05 to 30 mW. The large continuous current-induced blue-shift (much larger than the thermal energy k_BT) cannot be explained in terms of the usual band-to-band transitions. In order to describe the blue-shift behavior, we consider a band-filling effect for tails of the density of states (DOS), similar to that proposed earlier for heavily doped GaAs diodes [11]. GaN has been reported to manifest enhanced band-tailing [12], even comparable to that in amorphous Si. In InGaN, there is an additional source of inhomogeneous broadening, namely, fluctuations in alloy composition. The states in the band tails are formed in local potential minima, resembling QDs. Their origin could be assigned to various causes, such as composition fluctuations, high density of impurity states, inhomogeneous lattice deformations, etc. In GaN, the tails are likely associated with the high density of dislocations. In InGaN, additional (and perhaps dominant) contribution to tail formation may arise from fluctuations of In content, often observed in InGaN/GaN QW samples. Such phase segregation creates local potential fluctuations that are highly susceptible to rapid state filling as the excitation level is increased [13,14]. Therefore, this effect can be attributed to the rapid band filling of localized $In_xGa_{1-x}N$ radiative centers composed of large In concentrations.

On the other hand, the FWHMs of these spectra also increase from 36 to 49 meV for SQW sample, while broadening of linewidth from 67 to 74 meV for stair-shaped SQW, in the 0.05 to 30 mW range; since that the electron–phonon scattering mechanism contributes to the monotonic broadening with excitation power increase, as indicated in Fig. 4. Recombination of electron–hole pairs in such self-formed QDs can be viewed as localized exciton recombination. A random nature of these InGaN QD-like nanostructures would explain the observed large spectral broadening of the emission band. Taking into account the electron/hole relaxation interactions apparently occurring, as discussed above, the rearrangement of the energy configuration inherently gives rise to significant changes in the occupied states of the interacting ensemble. Upon

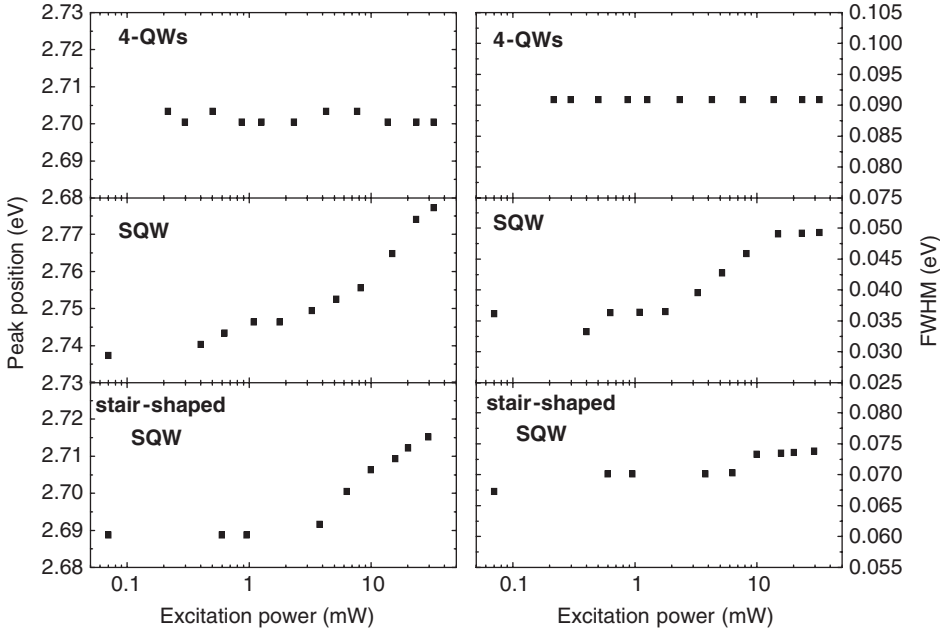

Fig. 4. The excitation power dependence of the emission peak position and FWHM of the three samples.

approaching thermodynamic equilibrium, the photocarrier thermalization process arising from the carriers relaxes favorably to adjacent trapping centers, with varied localization potentials, which determines the inhomogeneous line broadening. However, due to the inhibition of the carrier transfer and strongest localization effect, stair-shaped SQW with wider interdot spacing, exhibits more excitation insensitivity. All our PL measurements can be explained by carrier localization in a consistent way.

4. Summary

In summary, we have investigated the carrier localization of InGaN/GaN QW LEDs with different structures. Cross-sectional HAADF-STEM images observations revealed that the deep localization of excitons (or carriers) originates from the In-rich regions acting as QDs. From TD-PL and EPD-PL experiments, we can expect efficient luminescence in InGaN originates due to carriers' radiative recombination through localizing states. The fact that the localized energy depth depends on the structural parameters can be observed from our PL analysis. Generally speaking, stronger localization effect increases the higher internal quantum efficiency at room temperature. Furthermore, the deeper localized potential fluctuations are highly susceptible to rapid state filling as the excitation level is increased.

Acknowledgements

This work was partially supported by the National Science Council of the Republic of China. We would like to thank Professor C.C. Yang of the National Taiwan University for his help and support on the PL experiments.

References

[1] S. Chichibu, K. Wada, S. Nakamura, Appl. Phys. Lett. 71 (1997) 2346.
[2] M.G. Cheong, C. Liu, H.W. Choi, B.K. Lee, E.K. Suh, H.J. Lee, J. Appl. Phys. 93 (2003) 4691.
[3] H.K. Cho, J.Y. Lee, C.S. Kim, G.M. Yang, N. Sharma, C. Humphreys, J. Crystal Growth 231 (2001) 466.
[4] M.S. Jeong, J.Y. Kim, Y.W. Kim, J.O. White, C.H. Suh, C.H. Hong, H.J. Lee, Appl. Phys. Lett. 79 (2001) 976.
[5] S.F. Chichibu, A.C. Abare, M.S. Minsky, S. Keller, S.B. Fleischer, J.E. Bowers, E. Hu, U.K. Mishra, L.A. Coldren, S.P. DenBaars, T. Sota, Appl. Phys. Lett. 73 (1998) 2006.
[6] E. Berkowicz, D. Gershoni, G. Bahir, E. Lakin, D. Shilo, E. Zolotoyabko, A.C. Abare, S.P. Denbaars, L.A. Coldren, Phys. Rev. B 61 (2000) 10994.
[7] M.S. Minsky, S. Watanabe, N. Yamada, J. Appl. Phys. 91 (2002) 5176.
[8] S. Dhar, U. Jahn, O. Brandt, P. Waltereit, K.H. Ploog, Appl. Phys. Lett. 81 (2002) 673.
[9] T. Yamamoto, M. Kasu, S. Noda, A. Sasaki, J. Appl. Phys. 68 (1990) 5318.
[10] R.A. Street, T.M. Searle, I.G. Augustein, in: J. Stuke, W. Brenig (Eds.), Amorphous and Liquid Semiconductors, Taylor and Francis, London, 1974, p. 953.
[11] P.G. Eliseev, M.A. Man'ko, A.I. Krasil'nikov, I.Z. Pinsker, Phys. Status Solidi 23 (1967) 587.
[12] C.H. Qiu, C. Hoggatt, W. Melton, M.W. Leksono, J.I. Pankove, Appl. Phys. Lett. 66 (1995) 2712.
[13] S. Chichibu, T. Azuhata, T. Sota, S. Nakamura, Appl. Phys. Lett. 69 (1996) 4188.
[14] X. Zhang, D.H. Rich, J.T. Kobayashi, N.P. Kobayashi, P.D. Dapkus, Appl. Phys. Lett. 73 (1998) 1430.